



LAWRENCE
LIVERMORE
NATIONAL
LABORATORY

Laser damage initiation and growth of antireflection coated S-FAP crystal surfaces prepared by pitch lap and magnetorheological finishing

C. J. Stolz, J. A. Menapace, K. I. Schaffers, C. Bibeau, M. D. Thomas, A. J. Griffin

November 8, 2005

Boulder Damage Symposium
Boulder, CO, United States
September 19, 2005 through September 21, 2005

Disclaimer

This document was prepared as an account of work sponsored by an agency of the United States Government. Neither the United States Government nor the University of California nor any of their employees, makes any warranty, express or implied, or assumes any legal liability or responsibility for the accuracy, completeness, or usefulness of any information, apparatus, product, or process disclosed, or represents that its use would not infringe privately owned rights. Reference herein to any specific commercial product, process, or service by trade name, trademark, manufacturer, or otherwise, does not necessarily constitute or imply its endorsement, recommendation, or favoring by the United States Government or the University of California. The views and opinions of authors expressed herein do not necessarily state or reflect those of the United States Government or the University of California, and shall not be used for advertising or product endorsement purposes.

Laser damage initiation and growth of antireflection coated S-FAP crystal surfaces prepared by pitch lap and magnetorheological finishing

Christopher J. Stolz^a, Joseph A. Menapace^a, Kathleen I. Schaffers^a, Camille Bibeau^a,
Michael D. Thomas^b and Andrew J. Griffin^b

^aUniversity of California, Lawrence Livermore National Laboratory,
7000 East Avenue L-491, Livermore, CA 94550

^bSpica Technologies Inc., 18 Clinton Drive #3, Hollis, NH 03049

ABSTRACT

Antireflection (AR) coatings typically damage at the interface between the substrate and coating. Therefore the substrate finishing technology can have an impact on the laser resistance of the coating. For this study, AR coatings were deposited on Yb:S-FAP [Yb³⁺:Sr₅(PO₄)₃F] crystals that received a final polish by both conventional pitch lap finishing as well as magnetorheological finishing (MRF). SEM images of the damage morphology reveals laser damage originates at scratches and at substrate coating interfacial absorbing defects.

Previous damage stability tests on multilayer mirror coatings and bare surfaces revealed damage growth can occur at fluences below the initiation fluence. The results from this study suggest the opposite trend for AR coatings. Investigation of unstable HR and uncoated surface damage morphologies reveals significant radial cracking that is not apparent with AR damage due to AR delamination from the coated surface with few apparent cracks at the damage boundary. Damage stability tests show that coated Yb:S-FAP crystals can operate at 1057 nm at fluences around 20 J/cm² at 10 ns; almost twice the initiation damage threshold.

Keywords: Antireflection coating, e-beam, Yb:S-FAP, damage growth, damage morphology, MRF, HfO₂, SiO₂

1. INTRODUCTION

The compactness of the diode-pumped Mercury laser amplifier relies on near normal incidence, closely stacked Yb:S-FAP slabs¹⁻² in a helium gas-cooled environment³. Because the slabs are used at normal incidence, they require an antireflection (AR) coating to minimize transport losses, maximize pump light absorption, suppress ASE buildup and minimize ghost reflections. The Mercury laser operates at 10 Hz, 3-10 ns, and 1047 nm with a nominal crystal aperture of 4 cm × 6 cm. The design output energy for Mercury is 100 J/pulse (1 kW average power) with current operations at 50 J/pulse. AR coated optical surfaces often limit the fluence of transmissive laser optics. Because of the high helium cooling flow (0.1 Mach) and extensive handling of the crystals during mounting, laser-resistant sol gel coatings are an impractical technology due to their fragility. Instead, mechanically robust, but lower damage fluence e-beam coatings were selected for this application. In order to determine the maximum safe operating fluence for these crystals in the event that some laser damage did occur, laser damage stability tests were conducted.

Traditionally the S-FAP crystals have been lap finished, however, the process of bonding together crystal halves into a single optic has created transmitted wavefront errors that are uncorrectable without a small-tool finishing technique. MRF was successfully demonstrated to correct the transmitted wavefront errors necessitating determination of the impact of this finishing technique on AR coating damage and growth threshold.

2. DAMAGE MORPHOLOGY VERSUS SURFACE FINISHING TECHNIQUE

The damage test set-up used for these experiments is described elsewhere in this proceedings.⁴ The damage tester uses a Q-switched 1064-nm Nd:YAG laser with a 3.5-ns pulsewidth and 10-Hz repetition rate. The 1/e² beam diameter is

nominally 1 mm. The AR coatings have a dual wavelength requirement ($<0.2\%T$ at 900 and 1047 nm) for the diode pump and operating laser respectively. The coatings consist of hafnia and silica with a half-wave overcoat and undercoat (barrier layer) of silica to improve laser resistance.⁵

Carniglia⁶ describes AR coating laser damage as interfacial damage between the coating and substrate initiated by small diameter ($<0.1\ \mu\text{m}$) absorbing defects imbedded in cracks in the surface or subsurface. These nano-scale absorbers could be the result of polishing or contamination due to inadequate cleaning before coating. Carniglia further describes a damage model that is illustrated in figure 1. The absorber, when exposed to a laser beam of sufficient energy, creates a plasma which causes a buckling or blistering of the coating from the optical surface. At the edges of the blister, the coating stress is highly tensile allowing fractures and hence delamination of the coating. This coating damage morphology is also very similar to flat bottom pits in multilayer high reflector coatings where Dijon⁷ develops a similar damage initiation model based on a nanometer size absorber at the interfaces with highest standing wave electric fields. Laser damage studies by Papernov⁸ of 50-nm gold spheres imbedded between a silica overcoat and fused silica surface clearly illustrate that nano-sized absorber of this size can easily create plasmas and laser damage.

If nano-absorbers do indeed initiate surface laser damage, then the initial onset of bare surface damage would be extremely small micropitting. Because of the delamination morphology with AR coatings, the damage size is magnified significantly for damaged AR coatings. If the nano-sized absorber originated from polishing and inadequate cleaning before coating, one could hypothesize that the damage threshold of AR coated and uncoated surfaces would be equivalent, however, the scale of the damage size would be different. Therefore, for damage systems with inadequate detection sizes, uncoated surfaces would appear to have a higher laser damage threshold.

Damage test results (Fig. 2) show a significant fluence range for equivalent damage probabilities for coated versus uncoated S-FAP with a damage size detection limit of approximately $5\ \mu\text{m}$. There also appears to be a dependence of laser resistance on the finishing technique used for coated S-FAP crystals with conventional pitch lap finishing yielding the highest laser resistance. Interestingly, as discussed in section 3, there appears to be little difference in the AR damage growth threshold regardless of the finishing process.

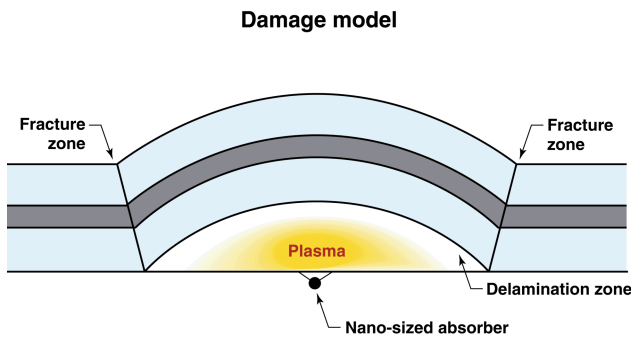


Fig. 1 Irradiated nano-absorber creates plasma leading to delamination of AR coatings.

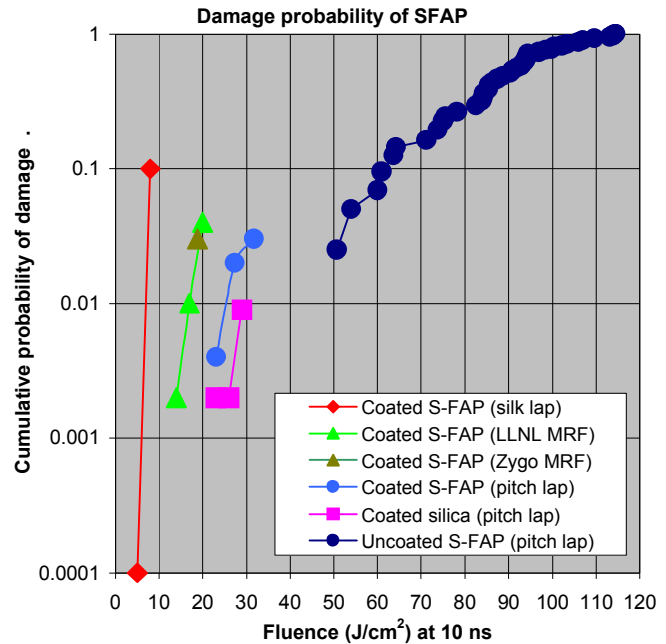


Fig. 2 AR-coating damage probability curves for various finishing techniques compared to uncoated S-FAP illustrate the impact of finishing on AR damage threshold. The coatings were manufactured in the same run.

2.1 CONVENTIONAL PITCH LAP FINISH

S-FAP crystals are a fairly soft material that easily forms micro-surface scratches (“sleeks”) during polishing. Micrographs of AR-coating laser damage on pitch lap polished S-FAP crystals (Fig. 3) clearly illustrates that damage preferentially occurs at these micro-surface scratches, although damage did occasionally occur at unscratched locations. The coating conforms to surface imperfections such that surface scratches are replicated in the coating (see Fig. 3). Small (50 – 200 nm diameter), central pits are visible along the micro-surface scratches. The smoothness of the pits indicates melting in the presence of a plasma, consistent with the theory of nano-sized absorbers imbedded in scratches that are heated during laser exposure. The presence of surface ripples suggests shock waves or plasma interference melted into the surface during the damage event. The circular geometry of the coating damage pit is consistent with a delamination mechanism initiated by a central nano-sized absorber. Unlike the central image in figure 3, the majority of the damage sites observed had no apparent radial cracks suggesting a benign stable damage morphology. Cracks in optical materials may cause electromagnetic field enhancements, or absorbing broken bonds which could lead to reduction of the damage growth threshold.⁹

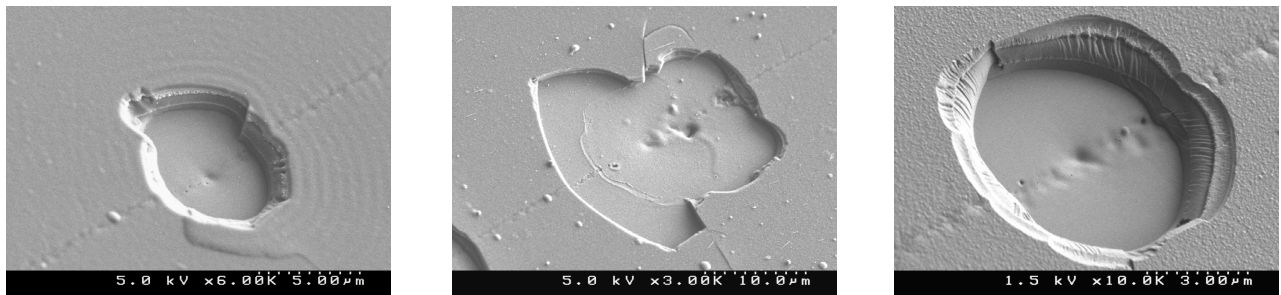


Fig 3. SEM images of AR-coating damage on a conventionally pitch-lap-finished S-FAP crystal showing damage along micro-fractures.

2.2 MRF FOLLOWING CONVENTIONAL PITCH LAP FINISH

Previous experiments on fused silica showed that surfaces prepared by MRF significantly reduced subsurface damage and when properly processed also significantly reduced the density of laser damage at 351 nm.¹⁰ Part of the post processing required for the high 351-nm laser resistance is acid etching to remove any imbedded iron (from the magnetically active MRF fluid) which is highly absorptive in the ultraviolet and IR. Inspection of the MRF S-FAP surfaces shows the absence of micro-surface scratches which were clearly visible on S-FAP crystals that were only pitch polished on a lap.

Examples of AR-coating damage on a S-FAP crystal conventionally lap polished on pitch followed by MRF are shown in figure 4. Although the AR-coating damage for surfaces prepared by these two different polishing processes is very similar (delamination with a central pit indicating an absorbing nano-sized absorbers), inspection of the left and central images reveals a different substrate damage morphology. Radial cracks and deep pitting (central image only) within the crystal suggest that the nano-sized absorbers might be more deeply imbedded than the nano-sized absorbers defects ejected from surface micro-surface scratches (Fig. 3).

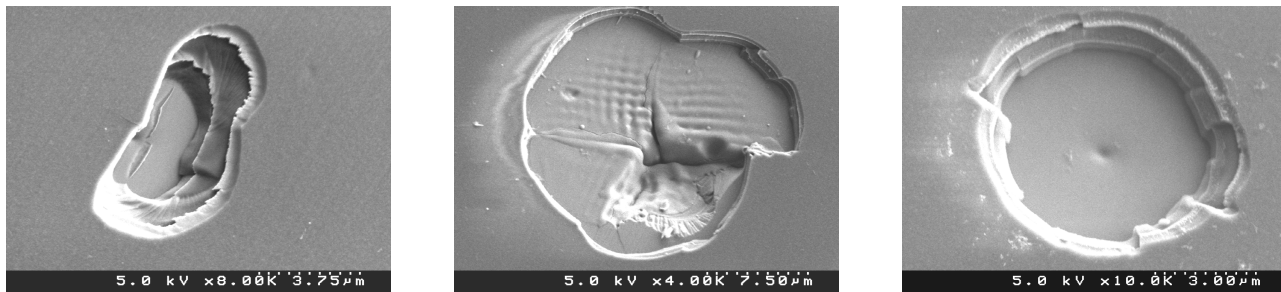


Fig 4. SEM images of AR damage a S-FAP crystal initially conventionally finished on a pitch lap with final figuring accomplished by MRF.

3. DAMAGE GROWTH

AR coating damage growth was assessed by first creating laser damage at a fluence above the initiation threshold to guarantee the creation of damage. On the conventionally polished S-FAP crystals, the test beam was aligned to a micro-surface scratch in order to increase the probability of damage. Sites on the MRF polished sample were selected randomly. Two initiation fluences were used, 15 and 20 J/cm² respectively, to determine potential growth threshold differences as a function of initiation fluence. For the limited number of test sites and over the initiation fluences used, no correlation between growth and initiation threshold were observed. Nor was there a correlation between number of initiated sites per unit area and the fluence used to create damage for this small range of test sites.

After damage initiation, the sample was exposed to a cumulative series of 1, 100, and 1000 shots at 15 J/cm² with microscopic inspection after each shot group to determine initiation of any new damage and stability of existing damage. In addition to the post microscopic inspection, a low magnification scatter diagnostic was used during laser exposure to detect rapid damage growth and terminate the test. If no damage growth was detected, the fluence was increased by 2.5 J/cm² and the shot sequence was repeated. This process continued until a fluence was reached where damage growth occurred. The results of these tests are illustrated in figure 5.

In summary, for the six areas that were tested with a range of 1-15 damage sites per 0.01-mm² test area, all damage was stable up to 20 J/cm². Once exposed to a fluence exceeding 20 J/cm², there was a probability that at least one of the damage sites per test area would grow with 5 of the 6 sites experiencing growth by 30 J/cm². Some of the damage growth was minor, while some of the growth was catastrophic forcing early termination of the test before the shot sequence was completed. Additionally, the catastrophic damage growth only became limited by the spot size of the test laser.

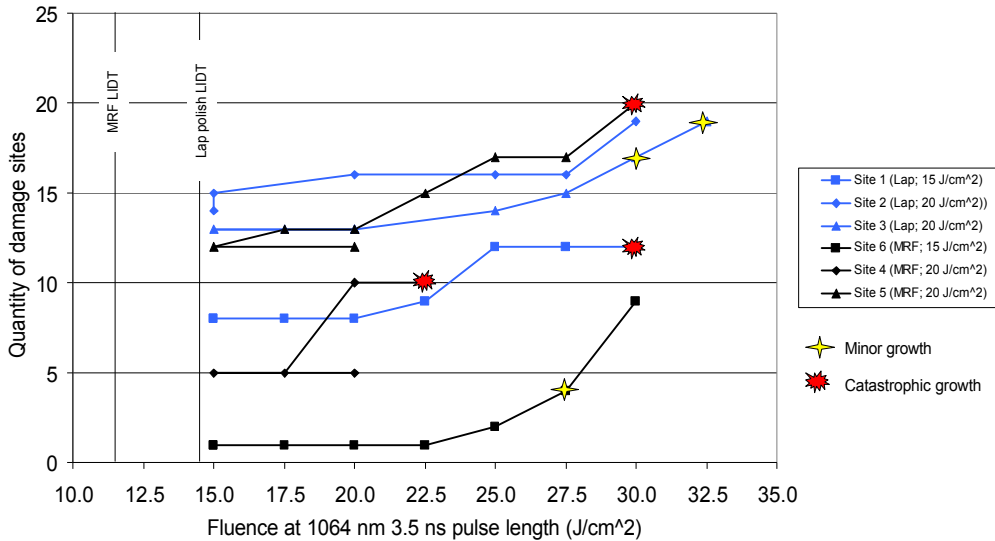


Fig 5. AR-coating damage density and fluence for damage growth on-site. The on-set of growth generally occurs between 20 to 30 J/cm², a fluence range about 2x higher than the initiation threshold (11-14 J/cm²). Neither the S-FAP finishing technique or initiation fluence (15 versus 20 J/cm²) has a significant impact on the AR-coating growth threshold.

3.1 CONVENTIONAL PITCH LAP FINISH

Microscope images of AR-coating initiation damage and growth from one test area on a conventionally pitch polished S-FAP crystal is shown in figure 6. Only images where changes occurred are shown. Damage was initiated at 15.5 J/cm² with no change to the surface with subsequent 1000-shot sequences at 17.5 and 20 J/cm². A new site (#1) was observed

on the micro-surface scratches after 1000 shots at 22.5 J/cm^2 . Two additional sites (2 and 3) were observed on the micro-surface scratch at 25 J/cm^2 as well as a new site (4) not affiliated with a visible micro-surface scratch. Catastrophic growth occurred at 25 J/cm^2 ; the test terminated at 1000 shots.

Because of the extensive damage growth, it is not possible to determine whether a new or existing damage site lead to the damage growth. For this particular series, however, site 2 remains relatively unchanged so is an unlikely candidate for the growth initiator.

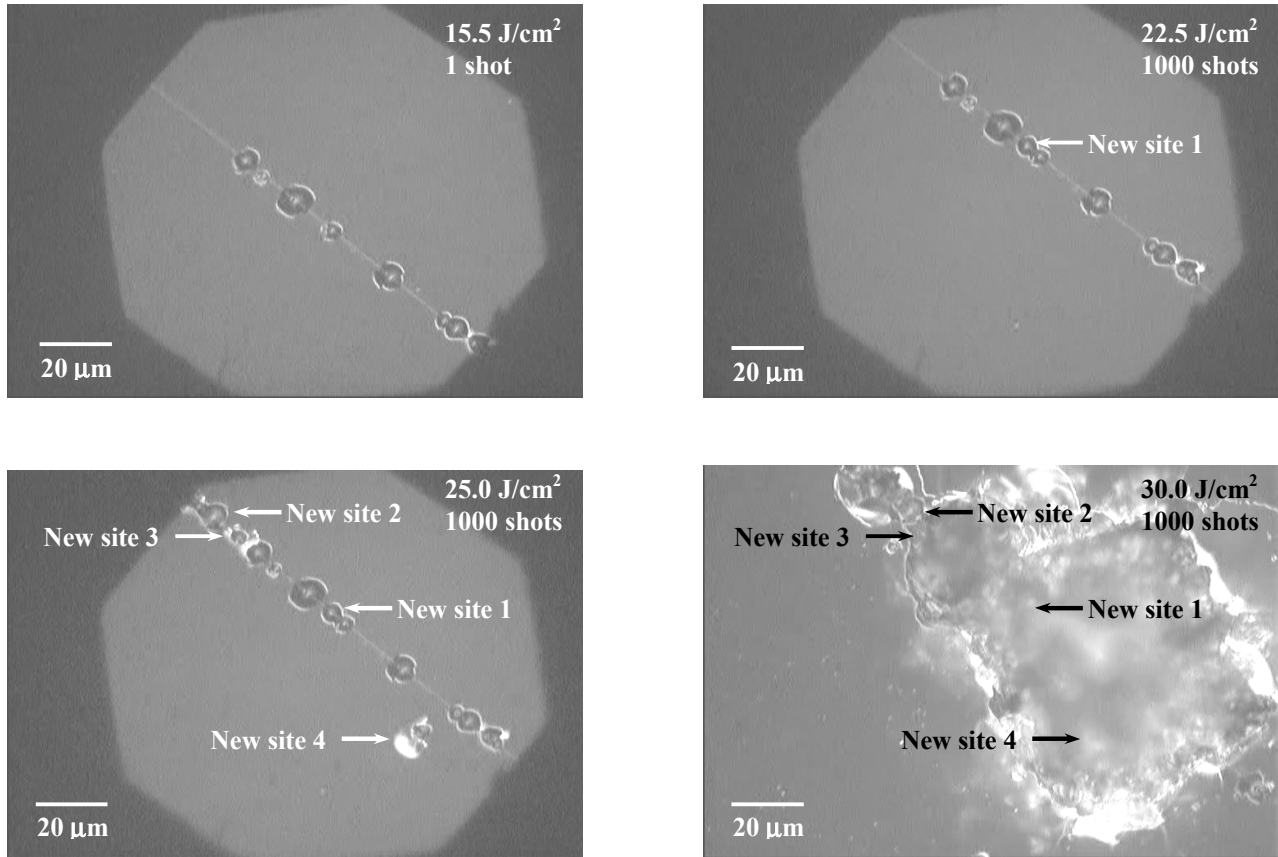


Fig 6. Optical micrographs of a typical laser damage growth test sequence of AR coated conventionally pitch-lap finished S-FAP crystal starting with initiation (top left) and ending with catastrophic growth (bottom right).

3.2 MRF FOLLOWING CONVENTIONAL PITCH LAP FINISH

Figure 7 illustrates a typical AR damage growth sequence for the sample that was first polished on a conventional pitch lap and then post polished using MRF. Damage was initiated at 20 J/cm^2 . The damage was randomly distributed across the surface unlike the non-MRF finished surface described above which had damage preferentially along micro-surface scratches. The fluence was reduced to 15 J/cm^2 with no visible newly initiated sites or damage growth. After increasing the fluence in 2.5 J/cm^2 increments catastrophic damage growth occurred at 22.5 J/cm^2 with the test being terminated after ~ 250 instead of 1000 shots. Tests of other areas showed damage growth at fluences of 27.5 and 30 J/cm^2 .

For the limited number of test areas, it does not appear to be advantageous to post process S-FAP slabs with MRF from a laser damage perspective without a post-processing step to remove any imbedded iron. Therefore, full-aperture Mercury slabs that do not require transmitted wavefront correction have no post MRF processing.

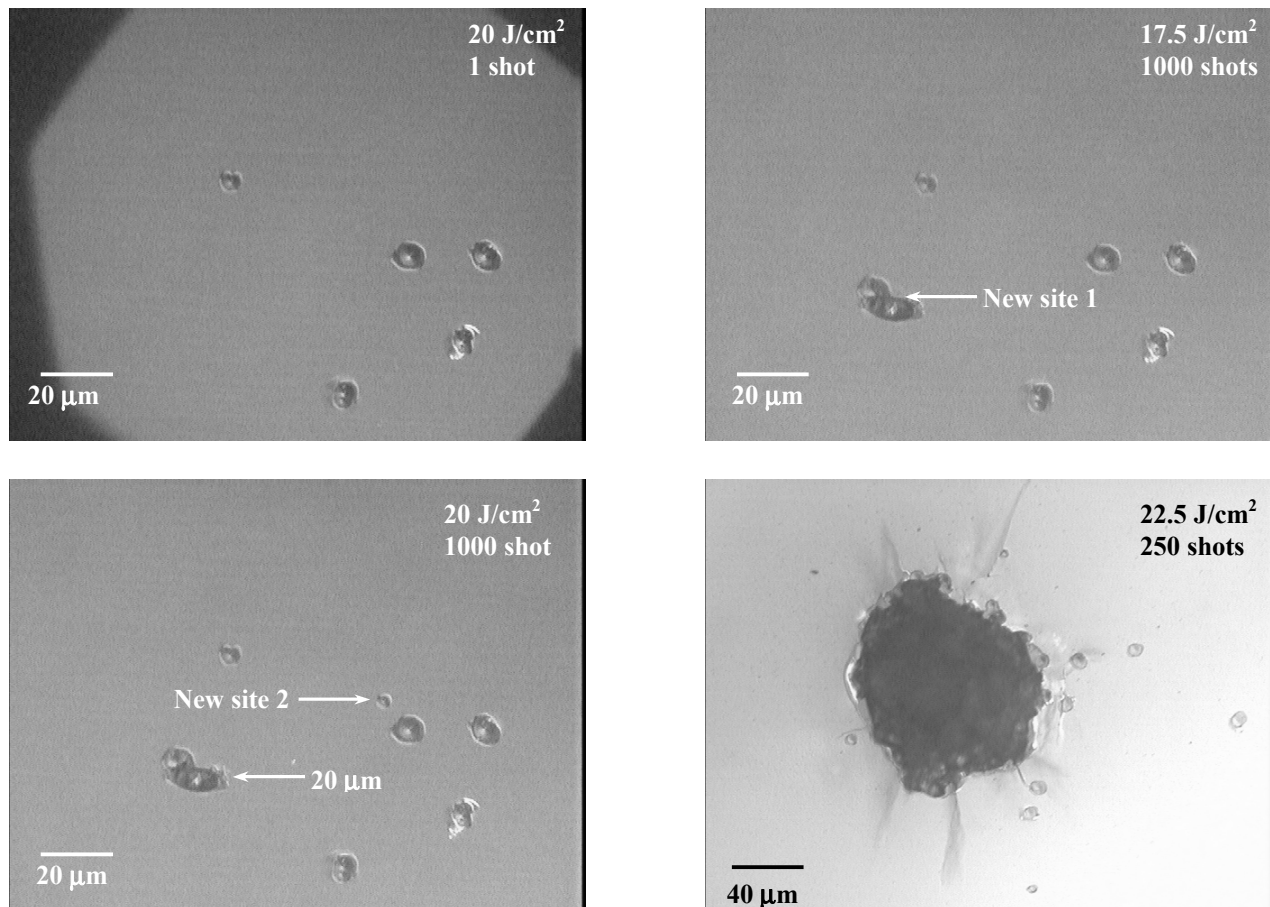


Fig 7. Optical micrographs of a typical laser damage growth test sequence of an AR coating on a S-FAP crystal surface treated with MRF and applied over a conventionally pitch-lap-finished surface.

4. CONCLUSIONS

Antireflection coating damage on S-FAP crystals is an interfacial morphology that appears to initiate at nano-absorbers imbedded within scratches in the surface and or subsurface. Once the initiator is exposed to the laser, a plasma is created causing the film to delaminate and fracture off of the surface. This process leads to a minimal amount of radial cracking suggesting a growth threshold higher than the initiation threshold. Experimental results collaborate this conclusion for coated S-FAP surfaces that are prepared by either a conventional pitch lap alone or post processed with MRF. Interestingly the MRF process removes the micro-surface scratches that are prevalent with the conventional pitch lap polishing process that harbor the nano-sized absorbers that thus cause AR coating damage, yet has a slightly lower damage threshold, likely due to the presence of iron in the surface.

ACKNOWLEDGEMENTS

The authors would like to acknowledge the support of Alene Clasen and Clayton Dahlen in preparing the figures and manuscript. The authors would also like to acknowledge the contributions of Karl George and team at Quality Thin Films, Inc. for depositing the optical coatings. This work was performed under the auspices of the U. S. Department of Energy by the University of California, Lawrence Livermore National Laboratory under Contract No. W-7405-Eng-48.

REFERENCES

1. K. I. Schaffers, J. B. Tassano, A. J. Bayramian, J. W. Dawson, C. Bibeau, S. A. Payne, R. C. Morris, M. H. Randles, A. DeWald, J. Rankin, and M. R. Hill, "High-quality, 4x6 cm² Yb:S-FAP [Yb³⁺:Sr₅(PO₄)₃F] crystal slabs for the Mercury laser", OSA Trends in Optics and Photonics on Advanced Solid State Lasers, Ed. J. J. Zayhowski (January 2003 Conference) Volume 83, p. 273.
2. K. I. Schaffers, "Yb:S-FAP [Yb³⁺:Sr₅(PO₄)₃F] Lasers", (The 3rd International Symposium on Laser and NLO Materials) **Optical Materials**, 26 (4): 391-394 Sept. 2004
3. C. Bibeau, A. J. Bayramian, R. J. Beach, R. W. Campbell, A. DeWald, W. H. Davis, J. W. Dawson, L. E. Dimercurio, C. A. Ebberts, B. L. Freitas, M. R. Hill, K. M. Hood, V. K. Kanz, J. A. Menapace, S. A. Payne, M. H. Randles, J. E. Rankin, K. I. Schaffers, C. J. Stolz, J. B. Tassano, S. J. Telford, and E. J. Utterback, "Initial operation of the Mercury laser – A gas cooled, 10 Hz, Yb:S-FAP system", in Solid State Lasers XIII: Technology and Devices, R. Scheps and H. J. Hoffman, eds., Proc. SPIE 5332, 244-250 (2004).
4. M. R. Borden, J. A. Folta, C. J. Stolz, J. R. Taylor, J. E. Wolfe, A. J. Griffith, and M. D. Thomas, "Improved method for laser damage testing coated optics", to be published in this proceedings.
5. J. H. Apfel, E. A. Enemark, D. Milam, W. L. Smith, and M. J. Weber, "The effects of barrier layers and surface smoothness on 150-ps, 1064-nm laser damage of AR coatings on glass", Nat. Bur. Stand (U.S.), Spec. Publ. **509**, 255-259 (1978).
6. C. K. Carniglia, "Oxide coatings for one micrometer laser fusion", Thin Solid Films 77, 225-238 (1981).
7. J. Dijon, M. Poulingue, J. Hue, "Thermomechanical model of mirror laser damage at 1.06 μm. Part 2: flat bottom pits formation", in *Laser-Induced Damage in Optical Materials: 1998*, G. J. Exarhos, A. H. Guenther, M. R. Kozlowski, K. L. Lewis, and M. J. Soileau, eds., Proc. SPIE Eng. **3578**, 398-407 (1999).
8. S. Papernov and A. W. Schmid, "High-spatial-resolution studies of UV-laser-damage morphology in SiO₂ thin films with artificial defects", in *Laser-Induced Damage in Optical Materials: 2004*, G. J. Exarhos, A. H. Guenther, N. Kaiser, K. L. Lewis, M. J. Soileau, and C. J. Stolz, eds., Proc. SPIE **5647**, 141-155 (2005).
9. F. Y. Génin, A. Salleo, T. V. Pistor, and L. L. Chase, "Role of light intensification by cracks in optical breakdown on surfaces", J. Opt. Soc. Am. A 18, 2607-2616 (2001).
10. J. A. Menapace, B. Penetrante, D. Golini, A. Slomba, P. E. Miller, T. Parham, M. Nichols, and J. Peterson, "Combined advanced finishing and UV-laser conditioning for producing UV-damage-resistant fused silica optics", in *Laser-Induced Damage in Optical Materials: 2001*, G. J. Exarhos, A. H. Guenther, K. L. Lewis, M. J. Soileau, and C. J. Stolz, eds., Proc. SPIE **4679**, 56-67 (2002).